DOI: 10.1002/chem.200501548

Photoinduced Electron Transfer in α-Cyclodextrin-Based Supramolecular Dyads: A Free-Energy-Dependence Study

Bijitha Balan and Karical R. Gopidas*[a]

Abstract: Photoinduced electron transfer (PET) between α-cyclodextrin-appended pyrene (PYCD) and a few acceptor molecules was studied in aqueous solutions. The pyrene moiety in PYCD is located above the narrower rim of the α-CD and is fully exposed to water. The acceptors are monocyclic organic molecules and, upon dissolution in water in the presence of PYCD, a fraction of the donor–acceptor systems is present as supramolecular dyads and the remaining fraction as free molecules. Free-energy-dependence studies showed that electron transfer in the supramolecular dyads follows the Marcus equation. The donor–acceptor coupling and the reorganization energy were determined from fits of the data to the Marcus equation. The electronic coupling was found to be similar to those reported for hydrogen-bonded systems. It appears that the actual λ_{out} values are somewhat lower than values calculated with the continuum model. The experimental design has also allowed, for the first time, a visual demonstration of the inverted region on the basis of the raw fluorescence lifetime data.

Keywords: cyclodextrins · donor–acceptor systems · electron transfer · fluorescence quenching · supramolecular dyads

Introduction

During the last decade, a large number of noncovalently bound donor–acceptor systems was designed and studied both as models for the naturally occurring photosynthetic reaction centers and also to explore unnatural systems for light harvesting.[1] Hydrogen bonding, π-stacking, and metal–ligand coordination are the noncovalent interactions often exploited to assemble donor–acceptor systems for this purpose. Although modest success has been achieved with these systems, they suffer from the disadvantage that the noncovalent assembly involving these interactions generally occurs in nonaqueous solutions. A better approach to mimic the biological systems is to build the donor–acceptor assembly in aqueous solutions by means of hydrophobic interactions. Examples of such studies include photoinduced electron transfer in peptides, nucleic acids, micelles, and other related systems.[2] In this context, water-soluble host–guest systems based on cyclodextrins (CDs) are increasingly being used to study and model various aspects of photoinduced energy and electron-transfer reactions in aqueous environments.[3]

CDs are cyclic oligosaccharides with hydrophobic cavities capable of encapsulating suitably sized organic molecules from aqueous solutions.[4] CDs are ideal molecular receptors to build water-soluble supramolecular functional systems. The commonly available CDs, namely α-, β-, and γ-CDs have, respectively, six, seven, or eight D-glucopyranose units linked by α-(1,4) linkages. These are shaped like truncated cones with the primary hydroxy groups arranged around the narrow rim of the cone and the secondary hydroxy groups assembled on the wider rim. A very important attribute of CDs is that they are transparent to UV and visible light. Because of its water solubility, guest-encapsulation properties, and ability to mimic natural enzymatic systems, CDs are now increasingly being used in the design of supramolecular, photoinduced, electron-transfer systems. Although CDs have been used in the past as constrained media to carry out photochemical reactions,[5] the use of a CD as an assembler of donor–acceptor systems for photoinduced electron-transfer reactions emerged only recently. There are only a few examples of such systems reported in the literature.[6] Although these studies have established that electron transfer from a CD-appended chromophore to an encapsulated guest is feasible, several important aspects of electron transfer in these systems remain unaddressed. For example, the

[a] B. Balan, Dr. K. R. Gopidas
Photosciences and Photonics Section
Chemical Sciences and Technology Division
Regional Research Laboratory (CSIR), Trivandrum - 695019 (India)
Fax: (+91) 471-490-186
E-mail: gopidaskr@rediffmail.com

Supporting information for this article is available on the WWW under http://www.chemeurj.org/ or from the author.

magnitude of the electronic coupling between the CD-appended chromophore and the encapsulated guest, dependence of the electron-transfer rate on the free-energy change, and the influence of the CD cavity on the reorganization energy of the encapsulated guest are some of the important aspects that need to be studied. The present paper is an attempt to address some of these aspects.

Herein we describe a study of the free-energy dependence of the PET reaction between α-CD-appended pyrene (PYCD) and encapsulated acceptors. The reaction involves the excitation of the pyrene moiety to the singlet excited state followed by transfer of this electron to the acceptor encapsulated in the α-CD cavity. The reaction is performed in water so that these systems thus resemble the biological electron-transfer conditions more closely in which hydrophobic interactions play a very important role in holding the donor and acceptor at a proper distance and orientation. The acceptors selected are mono- or 1,4-disubstituted benzene derivatives and could lead to a ΔG^0 range of ≈ 0 to -1.5 eV. Because all the quenchers are monocyclic benzene derivatives, the reorganization energy associated with their one-electron reduction are expected to be similar. Thus the systems selected form a truly homogeneous series for a free-energy-dependence study.

Results and Discussion

Synthesis, characterization, and photophysical properties of PYCD: The strategy for the selective functionalization of the narrower rim of α-CD is well established in the literature,[7] and we employed this method to prepare PYCD (Scheme 1) in 30% yield. The structure of PYCD is assigned based on spectral evidence (see the Experimental Section). For example, the MALDI-TOF spectrum consists of only one peak at *m*/*z* 1209.2 that corresponds to $[PYCD+Na]^+$ (see Supporting Information). The peak corresponding to native CD is not observed. The extinction coefficient (calculated assuming a molecular weight of 1186) of the PYCD absorption maximum is very close to that of the unsubstituted pyrene, and this confirms that only one pyrene unit is attached to the CD ring. The regiochemistry was assigned based on a comparison of ^{13}C NMR chemical shifts with those in earlier reports (vide infra).

α-CD is built up of six glucose units, and PYCD has a pyrene attached to one of these glucose units. ^{13}C chemical shifts of the pyrene-attached glucose unit are expected to differ somewhat relative to those for unsubstituted glucose units; within the pyrene-attached glucose unit, ^{13}C chemical shifts are expected to vary depending on the position of attachment. When an alcohol is alkylated, the ^{13}C NMR chemical shifts of the α- and γ-carbon atoms are known to move downfield by approximately 10 and 1 ppm, respectively, and that of the β-carbon atom is known to move upfield by ≈2 ppm. D'Souza and co-workers[7a] used this argument to assign the regiochemistry of monosubstituted cyclodextrins. They assumed that, if C6-OH is substituted, the C_6 carbon is expected to shift downfield by ≈10 ppm, C5 is expected to shift upfield by ≈1 ppm, and C4 is expected to shift downfield by ≈0.3 ppm. There are five intense peaks in the carbohydrate region of the ^{13}C NMR spectrum of PYCD (see Supporting Information). Based on a comparison with the spectrum of α-CD and literature precedence, these intense peaks are assigned to the carbon atoms in the five unsubstituted glucose units at $\delta = 102.09$ (C1), 82.23 (C4), 73.45 (C3), 72.23 (C2 and C5), and 60.19 ppm (C6). In addition to this, there are eight smaller peaks. The small peak at $\delta = 71.02$ ppm is assigned to the CH_2 group attached to pyrene. Six of the remaining seven peaks can then be assigned to the six carbons in the pyrene-attached glucose ring. Of these, the peak at $\delta = 69.34$ is assigned to the C6 carbon and this signal is 9.15 ppm downfield from the normal value because of attachment to the pyrene unit. The other signals were: C5 at $\delta = 71.29$ (0.94 ppm upfield), C4 at 82.61 (0.4 ppm downfield), C3 at 73.05 (0.4 ppm upfield), C2 at 72.59 (0.36 ppm downfield) and C1 at 102.52 ppm (0.43 ppm downfield). Because the C6 signal is shifted by more than 9 ppm and C5 is shifted by nearly 1 ppm, this confirms that the pyrene is attached to the C6 carbon, which is on the narrower rim of α-CD. The above assignments are consistent with those given by D'Souza and co-workers.[7a]

A small signal at $\delta = 60.68$ ppm (0.49 ppm downfield from unmodified C6 signal) remains unaccounted. D'Souza and co-workers[7a] also observed such a peak, but they have not assigned it. When a relatively large molecule, such as pyrene, is attached to the narrower rim of α-CD, the CH_2OH groups projecting out of the narrower rim may experience steric crowding. This effect may be greater on adjacent glucose rings. In consideration of this, we tentatively assign this signal to the C6 carbon atoms of the glucose unit(s) adjacent to the one to which pyrene is attached.

Several examples of pyrene attached to γ-CD are reported in the literature and some of these are useful as sensors of organic molecules in aqueous solutions.[8] In these systems, pyrene is hosted by the γ-CD cavity. Because of its relatively large size, pyrene cannot be hosted in the cavities of α- and β-CDs.[9] Nevertheless, size considerations cannot rule out partial inclu-

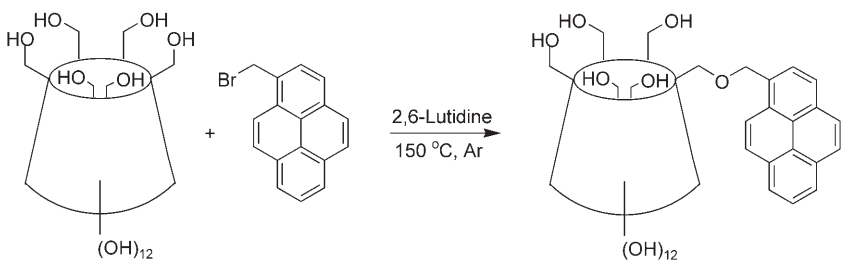

Scheme 1. Synthesis of PYCD.

sion of pyrene within the α-CD cavity in PYCD. Absorption and emission spectral studies described below, however, suggested that the pyrene moiety in PYCD is fully exposed to water.

The absorption and emission spectra of PYCD in water are shown in Figure 1. The absorption spectral profile and

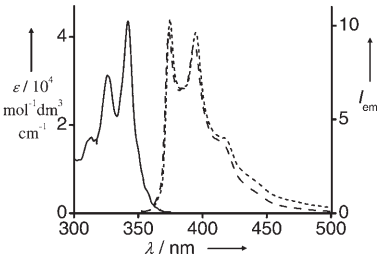

Figure 1. Absorption (——) and emission (– – –) spectra of PYCD in water, and the emission spectrum (-----) of 1-pyrenemethanol in water.

extinction coefficient of PYCD closely resemble those of pyrene in common solvents. This indicates that there is only negligible interaction between pyrene and α-CD moieties in PYCD. The emission spectrum of PYCD was superimposable on the emission spectrum of 1-pyrenemethanol in water (as shown by the dotted line in Figure 1), which again indicated that the pyrene moiety is fully exposed to water in the most stable conformation of PYCD. On the basis of the absorption and emission maxima, the excitation energy ($E_{0,0}$) of PYCD was calculated and the value obtained was 3.5 eV. The fluorescence decay of PYCD was monoexponential with a lifetime of 204 ns.

Interaction of acceptors with PYCD: The acceptor molecules employed in the study are 4-chlorobenzonitrile (CBN), dimethylterephthalate (DMP), 1,4-dicyanobenzene (DCB), acetophenone (ACP), benzaldehyde (BZA), nitrobenzene (NB), 4-chloronitrobenzene (CNB), and methyl-4-nitrobenzoate (MNB). Structures of the acceptor molecules are shown in Scheme 2. The reduction potentials of all these molecules are known in the literature[10] and the values are also given in Scheme 2. These molecules have been employed as acceptors in several photoinduced electron-transfer reactions. Earlier workers have documented photoinduced electron-transfer reactions between pyrene and most

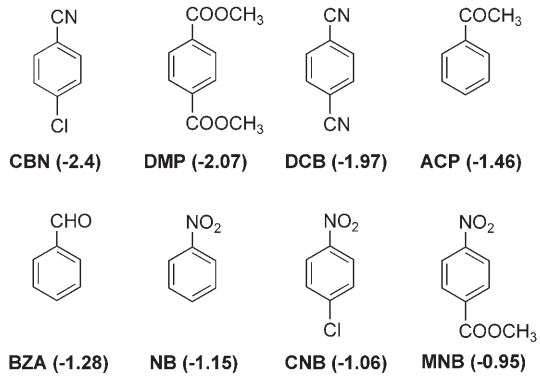

Scheme 2. Structures of acceptors used in the study. Reduction potentials [in V] versus SCE are given in parentheses.

of the quenchers listed in Scheme 2 by means of fluorescence quenching and laser flash-photolysis techniques.[11] Radical cations of pyrene and radical anions of most of the acceptors were also characterized in these studies thereby establishing that photoinduced electron-transfer takes place in these donor–acceptor systems. The onset of absorption for all these acceptors is below $\lambda = 320$ nm (see Supporting Information). This indicates that singlet energies of these molecules are higher than that of pyrene. Hence singlet–singlet energy transfer from pyrene to the acceptors would be endothermic and this eliminates the possibility of pyrene fluorescence being quenched by these acceptors by an energy-transfer mechanism.

Because of their smaller sizes, the monocyclic aromatics shown in Scheme 2 could easily be included in the small cavity of α-CD. In fact, inclusion behavior of several mono- and 1,4-disubstituted benzene derivatives in α-CD (including some molecules shown in Scheme 2), was studied both theoretically and experimentally.[12] These compounds were found to associate with α-CD in water with association constants (K_a) in the range 50–400 M^{-1}.

All the acceptor molecules were soluble in water in the 10^{-4}–10^{-3} M concentration range. Upon addition of the quenchers to aqueous PYCD solutions, the long wavelength absorption of PYCD remained unaffected (Figure 2a) indicating that the pyrene moiety in PYCD has no ground state interactions with the acceptors. On the other hand, the absorption spectra of the quenchers undergo slight changes

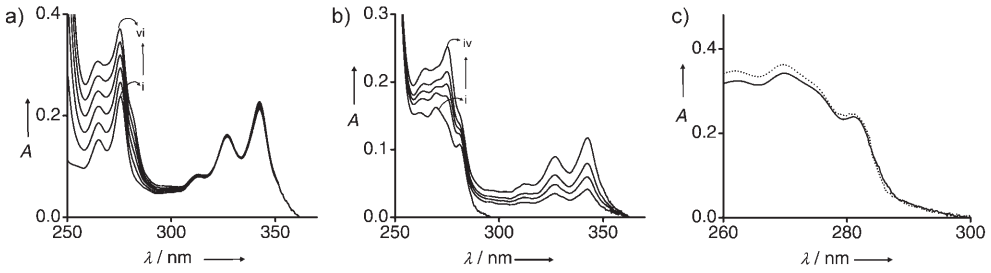

Figure 2. a) Changes in the absorption spectrum of PYCD (i) (5×10^{-6} M) with varying concentrations (8–40×10^{-4} M) of CBN (ii–vi); b) Changes in absorption spectrum of CBN (i) (4×10^{-4} M) with varying concentrations (1.0–2.5×10^{-6} M) of PYCD (ii–iv); c) Change in absorption spectrum of CBN (8×10^{-4} M) in the absence (——) and presence (-----) of native α-CD (1×10^{-5} M).

upon addition of small amounts of PYCD (Figure 2b). Because the pyrene moiety of PYCD also absorbs in the same region, the spectral shifts could not be analyzed to obtain K_a values. In Figure 2c, absorption spectra of one of the acceptors, CBN, in the absence and presence of native α-CD are presented, which clearly shows the association process.

Other quencher molecules also exhibited similar behaviors. Figure 2 seems to suggest that PYCD interacts with the quenchers, but the interactions are with the α-CD part of PYCD and the pyrene moiety remains unaffected by this interaction. Inclusion of the acceptors probably occurs through the wider rim of α-CD, which is away from the pyrene moiety. Park et al. have recently shown that encapsulation of guest molecules in CDs preferably takes place through the secondary face.[13]

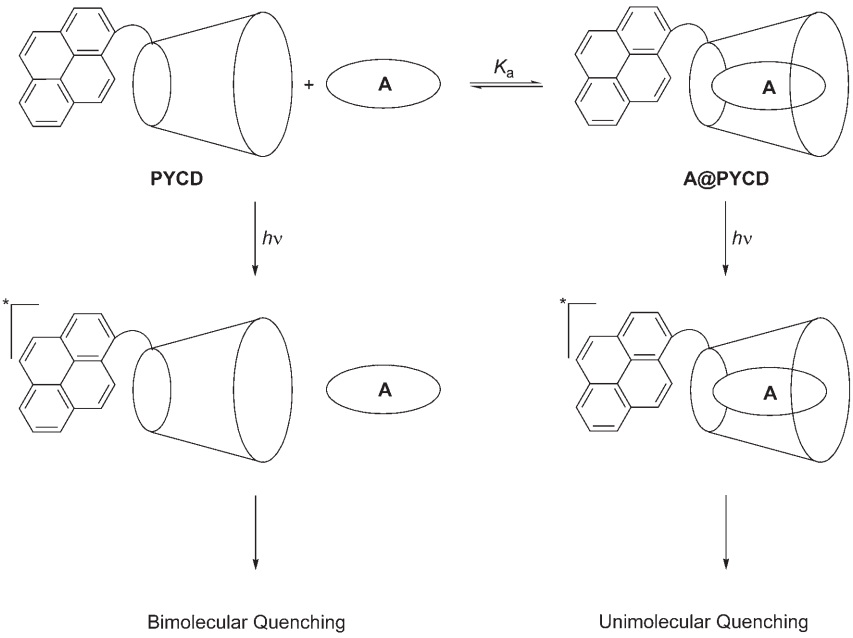

Scheme 3. Scheme showing unimolecular and bimolecular quenching pathways for α-CD-appended pyrene.

Fluorescence quenching: All the acceptors shown in Scheme 2 quench the fluorescence of PYCD in aqueous solutions. Figure 3 shows an example of this quenching in which the fluorescence intensity progressively decreases

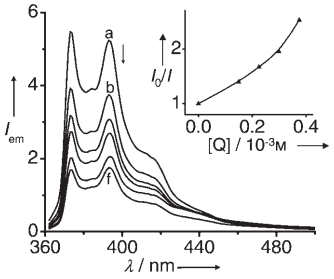

Figure 3. Fluorescence spectra of PYCD in the absence (a) and in the presence (b–f) of DCB. Concentration of DCB varied from $1–4\times10^{-4}$ M. Inset is a plot of I_0/I for this quenching.

with addition of increasing amounts of DCB. The I_0/I plot for the fluorescence quenching is shown in the insert in Figure 3 and shows an upward curvature at higher concentrations of the quencher, which indicates that two types of quenching are taking place in the system. Similar behaviors were also observed with other quenchers.

The model shown in Scheme 3 can explain the different types of quenching taking place in the PYCD/acceptor systems. Up on mixing acceptor A with PYCD in aqueous solutions, a fraction of A undergoes encapsulation in the cavity of PYCD to give A@PYCD and an equilibrium as shown in Scheme 3 is established. When irradiated, the pyrene moieties in free PYCD and A@PYCD are excited. As shown in Scheme 3, free *PYCD is quenched by free moving A molecules in a bimolecular, diffusion-mediated electron-transfer reaction. The excitation in A@*PYCD, on the other hand, is quenched by the encapsulated A, in a fixed-distance, unimolecular electron-transfer reaction. The unimolecular and bimolecular components of the electron-transfer reactions can be evaluated separately by fluorescence lifetime quenching experiments.

Fluorescence decay of PYCD was monoexponential in the absence of acceptors. Addition of an acceptor results in unimolecular and bimolecular quenching pathways and this leads to biexponential decays that can be expressed as in Equation (1), where τ_1 and τ_2 are defined by Equations (2) and (3), and $\chi_{(A@PYCD)}$ is the mole fraction of the encapsulated species, χ_{PYCD} is the mole fraction of free PYCD, k_0 (= $1/\tau_0$) is the intrinsic decay rate of the probe, k_{et} is the unimolecular rate constant of electron transfer within the encapsulated segment, k_q is the bimolecular quenching rate constant for the unassociated PYCD molecules and [A] is the concentration of the acceptor.

$$I_t = \chi_{(A@PYCD)}\exp(-t/\tau_1) + \chi_{(PYCD)}\exp(-t/\tau_2) \quad (1)$$

$$\tau_1 = (k_0 + k_{et})^{-1} \quad (2)$$

$$\tau_2 = (k_0 + k_q\tau_0[A])^{-1} \quad (3)$$

According to Equations (1)–(3), the short lifetime component (τ_1) is independent of the acceptor concentration and the long lifetime component (τ_2) is dependent on the acceptor concentration. From the short lifetime component, the

rate constant for electron transfer within the encapsulated complex A@PYCD can be calculated with Equation (4).

$$k_{et} = 1/\tau_1 - 1/\tau_0 \quad (4)$$

The quenching rate constant k_q for the bimolecular process can be obtained from the slope of the Stern–Völmer plot of τ_0/τ_2 vs acceptor concentration [Eq. (5)].

$$\tau_0/\tau_2 = 1 + k_q\tau_0[A] \quad (5)$$

According to Equation (5), a plot of τ_0/τ_2 versus acceptor concentration will give a straight line with $k_q\tau_0$ as the slope. Thus, the rate constants k_{et} and k_q can be obtained from the same set of experiments.

The equilibrium association constant, K_a for the encapsulation process shown in Scheme 3 can also be determined from these experiments. $\chi_{(A@PYCD)}$ and $\chi_{(PYCD)}$ values, obtained from fitting the lifetime data, are proportional to the concentrations of the associated and unassociated fractions, respectively. Since the concentration of the acceptor is large compared to that of the associated complex, we can write Equation (6).

$$K_a = \frac{\chi_{(A@PYCD)}}{\chi_{(PYCD)}[A]} \quad (6)$$

Thus a plot of $\chi_{(A@PYCD)}/\chi_{(PYCD)}$ versus [A] will be linear and gives K_a as the slope.

Fluorescence decays of PYCD were measured in the presence of several concentrations (10^{-4}–10^{-3} M) of all acceptors listed in Scheme 2. A representative example is shown in Figure 4, where the fluorescence decays of PYCD in the

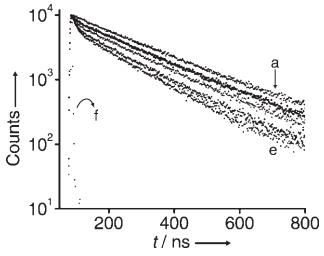

Figure 4. Fluorescence decay profiles of PYCD in the absence (a) and presence (b–e) of different concentrations (5–55 × 10^{-5} M) of DMP. Spectrum f is the lamp profile

presence of different concentrations of DMP are presented (decay curves for other systems are given in the Supporting Information). The biexponential nature of the decay is very evident from the figure. Analysis of the decay curves showed that: i) the short lifetime component τ_1 is independent of the acceptor concentration, ii) the relative contribution of τ_1 increases with acceptor concentration, and iii) τ_2 decreases with increase in acceptor concentration. We also noted that the short lifetime component disappears upon addition of methanol (15% by volume) to the above solutions. The role of methanol is to prevent the hydrophobic interaction between PYCD and acceptors, thereby preventing the encapsulation process. The unimolecular fluorescence-quenching component will be absent in this case.

We have obtained the fluorescence decay profiles for all PYCD–acceptor systems and the data were analyzed by Equation (1) (fit parameters such as τ_1, τ_2, $\chi_{(A@PYCD)}$, and $\chi_{(PYCD)}$ obtained for all systems are provided in the Supporting Information). The rate constants for electron transfer in the encapsulated systems k_{et} were calculated with τ_1 values obtained from the fits [Eq. (4)]. The intermolecular component of the decays were analyzed and plotted with Equation (5) to obtain straight-line plots. Representative examples are shown in Figure 5a. Plots of $\chi_{(A@PYCD)}/\chi_{(PYCD)}$ versus

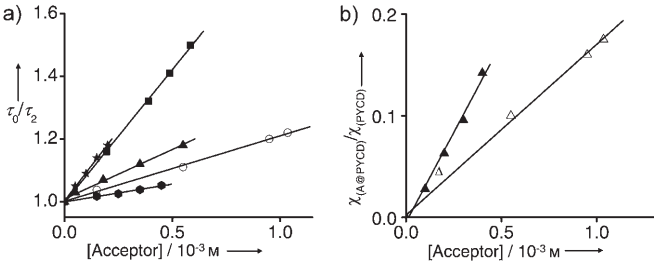

Figure 5. a) τ_0/τ_2 plot for the lifetime quenching of PYCD by CBN (●), DCB (○), DMP (▲), ACP (■) and MNB (★); b) plots of $\chi_{(A@PYCD)}/\chi_{(PYCD)}$ vs [Acceptor] for CNB (▲) and DCB (△).

acceptor concentrations were also made in all cases (see Figure 5b for some examples) and values of K_a were determined from these plots. Values of k_{et}, k_q, and K_a obtained by the analysis mentioned above are given in Table 1 for all systems.

Table 1. Free energies (ΔG^0), association constants (K_a), and rate constants (k_{et} and k_q) for the PYCD/acceptor systems.

Acceptor	K_a [M^{-1}]	ΔG^0 [eV]	k_q [$10^8 M^{-1}s^{-1}$]	k_{et} [10^7 s^{-1}]
CBN	145	−0.11	5.3	8.3 ± 0.3
DMP	193	−0.44	15.7	43.1 ± 2.0
DCB	140	−0.53	10.4	73.5 ± 2.5
ACP	179	−1.07	38.0	86.6 ± 3.8
BZA	461	−1.22	42.5	42.0 ± 0.9
NB	172	−1.35	42.9	7.1 ± 0.10
CNB	375	−1.44	42.8	3.0 ± 0.04
MNB	236	−1.55	44.0	2.0 ± 0.03

Electron-transfer rates: For nonadiabatic electron transfer involving weakly interacting donors and acceptors, the rate constant for electron transfer is given by the Marcus equation [Eq. (7)],[14] where $\hbar$ is Planck's constant divided by 2π, H_{el} is the coupling matrix element, λ is the reorganization energy, k_B is the Boltzmann constant, T is the absolute temperature and ΔG^0 is the free energy change for the electron-transfer reaction.

$$k_{et} = (2\pi\hbar^{-1})\, H_{el}^{\,2}\, (4\lambda k_B T)^{-1/2} \exp[-(\Delta G^0 + \lambda)^2/4\lambda k_B T] \quad (7)$$

The reorganization energy λ is the energy required to structurally reorganize the donor, acceptor and their solvation spheres upon electron transfer. Depending on the relative values of ΔG^0 and λ, Equation (7) envisages three typical kinetic regimes for electron-transfer reactions: i) a normal region ($\Delta G^0 > -\lambda$) where electron transfer is thermally activated and is favored by an increase in the driving force, ii) an "activation-less" regime ($\Delta G^0 = -\lambda$) where the rate is maximum, and iii) an "inverted region" for strongly exergonic reactions ($\Delta G^0 < -\lambda$), where the rate actually decreases with increase in driving force. The existence of an inverted region was the most important prediction of Marcus' theory. Although definitive evidence for its existence was lacking for a long time, the inverted region is now well-established in fixed-distance electron-transfer reactions.[15] Intermolecular electron-transfer reactions, where the donors and acceptors are allowed to diffuse freely, however, follow the pattern known as Rehm–Weller behavior, where the rate initially increases with driving force, reaches a maximum at which it remains as the driving force continues to increase.[16]

Free-energy dependence of electron-transfer rates: With redox potentials of pyrene and acceptors measured in acetonitrile, the free-energy change for electron-transfer ΔG^0 can be calculated with Equation (8),[17] where E_{ox} is the oxidation potential of the pyrene moiety in PYCD and E_{red} are the reduction potentials of the acceptors, r_P and r_A are the radii of the pyrene and acceptors units, respectively, ε_s is the dielectric constant of water, and d is the distance separating the pyrene and acceptor units.

$$\Delta G^0 = E_{ox} - E_{red} - E_{0,0} - \frac{e^2}{2}\left(\frac{1}{r_P} + \frac{1}{r_A}\right)\left(\frac{1}{37} - \frac{1}{\varepsilon_S}\right) - \frac{e^2}{\varepsilon_S d} \quad (8)$$

The oxidation potential of PYCD in water was measured as 0.9 V versus SCE. The reduction potentials of the acceptors, however, could not be measured in water because the reduction potentials of most of them lay outside the range possible in water. Hence we were forced to use the redox potentials of pyrene and the acceptors measured in acetonitrile or DMF and make the necessary corrections for the difference in solvation by means of the fourth term in Equation (8). We used $r_P = 3.6$ Å, $r_A = 3.5$ Å for monosubstituted benzenes, and $r_A = 4.0$–4.5 Å for disubstituted benzenes. These values were obtained with AM1 methods.[18] In order to calculate d, we assumed that the acceptors are centrally positioned in the α-CD cavity and that the midpoint of the pyrene moiety in PYCD is positioned ≈2 Å above the narrower rim of α-CD. This gives a d value of 6 Å for the intra-ensemble electron transfer. For diffusion-mediated electron transfer, d may be slightly different; however, the same values were assumed for the sake of simplicity. ΔG^0 values thus calculated are presented in Table 1. It can be seen that ΔG^0 values for the selected systems span a range of ≈0 to −1.5 eV.

Figure 6 is a plot of the bimolecular quenching rate constant, k_q versus ΔG^0. It can be seen that, as the driving force increases, k_q first increases, reaches a maximum, and then stays nearly invariant with further increases in the driving force. This is clearly an example of the Rehm–Weller behavior.

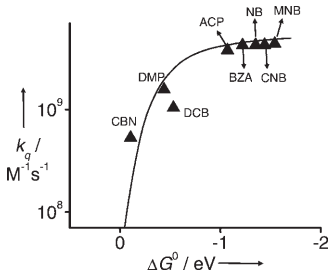

Figure 6. Plot of bimolecular quenching rate constants (k_q) versus ΔG^o. The solid line is a fit using Equation (9).

In the Rehm–Weller formalism, the overall quenching rate constant k_q in a bimolecular electron-transfer reaction is expressed by Equation (9),[16] where $\Delta G^{\#}$ is the free energy of activation for electron transfer and is given by Equation (10).

$$k_q = \frac{k_{diff}}{1 + 0.25[\exp(\Delta G^{\#}/RT) + \exp(\Delta G^0/RT)]} \quad (9)$$

$$\Delta G = \frac{\Delta G^0}{2} + \left[\left(\frac{\Delta G^0}{2}\right)^2 + (\Delta G_0{}^{\#})^2\right]^{1/2} \quad (10)$$

$\Delta G_0{}^{\#}$ in Equation (10) is the free energy of activation when there is no driving force for the reaction. We have assumed a value of 0.19 eV for $\Delta G_0^{\#}$. A value of 6.6×10^9 is normally used for the diffusion coefficient in this solvent. The fits obtained with these values are also shown in Figure 6. Notice that there is good agreement between the observed values and the calculated fit, which confirms that quenching of the CD-appended pyrene by free moving acceptors in solution, obeys the Rehm–Weller formalism.

Figure 7 is a plot of k_{et} versus ΔG^0. It can be seen from Figure 7 that as the driving force increases (i.e., ΔG^0 becomes more negative), k_{et} increases initially, reaches a maxi-

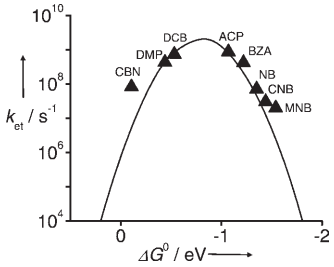

Figure 7. Plot of electron-transfer rate constant k_{et} versus ΔG^0. The solid curve is the computed curve of Equation (7).

mum, and then decreases. Thus we conclude that the intra-ensemble photoinduced electron transfer between the CD-linked pyrene and encapsulated acceptors follows Marcus-type behavior. The photoinduced electron transfer in CD-appended chromophores is thus similar to those in hydrogen-bonded systems, where the unimolecular component follows Marcus-type behavior and the bimolecular component obeys the Rehm–Weller pattern.[19]

Electronic coupling and reorganization energy: Our results show that photoinduced electron transfer in the supramolecular-CD dyads follows Marcus-type behavior (Figure 7). The data in Figure 7 can be fitted to Equation (7) to give H_{el} and λ values. We have attempted to fit the data to Equation (7) by means of various combinations of H_{el} and λ and the best fit was obtained for values of $H_{el} = 3\,cm^{-1}$ and $\lambda = 0.8\,eV$. The fit is also shown in Figure 7. Notice that there is good agreement between the observed values and the calculated fit, confirming the Marcus-type electron transfer taking place in these systems.

Although a few examples of photoinduced electron transfer in CD-appended systems are reported, values of H_{el} and λ have not been determined in any of these cases. Therefore, we are not able to compare our results with those in similar systems. The H_{el} values obtained are small, but similar to values reported for hydrogen-bonded donor–acceptor systems.[20] Considering the fact that the donor and acceptor are not linked directly and that they most probably have a through-space interaction, the low value obtained seems reasonable.

The reorganization energy λ obtained from the best fit is 0.8 eV. λ is the sum of inner shell (λ_{in}) and outer shell (λ_{out}) reorganization energies. λ_{out} is given by Equation (11),[21] where ε_{op} is the optical dielectric constant of the solvent.

$$\lambda_{out} = \Delta e^2\left(\frac{1}{2r_P}+\frac{1}{2r_A}-\frac{1}{d}\right)\left(\frac{1}{\varepsilon_{op}}-\frac{1}{\varepsilon_S}\right) \qquad (11)$$

This expression gave $\lambda_{out} = 0.7\,eV$. This suggested that λ_{in} is only 0.1 eV for these systems. This value of λ_{in} seems to be somewhat lower than expected. In our previous studies with hydrogen-bonded systems, we obtained $\lambda_{in} = 0.2\,eV$ for similar donor–acceptor systems.[19] Other groups also have used $\lambda_{in} = 0.2\,eV$ for small aromatic donor–acceptor systems.[20a] Because λ_{in} is solvent-insensitive, a similar value was expected here. We use the following argument to explain the low value calculated for λ_{in}. λ_{out} was obtained with Equation (11), and is the λ_{out} expected if both product ions are stabilized by solvation with water molecules. In the present systems, the pyrene moiety is fully exposed to water and the pyrene radical cation formed as a result of PET will be stabilized by solvation with water. However, the acceptor radical anions formed inside the α-CD cavity are not exposed to water molecules and hence they may not be stabilized by solvation. Thus the actual λ_{out} for the present systems will be somewhat less than the 0.7 eV obtained from Equation (11). If we assume that λ_{in} is 0.2 eV, then λ_{out} will turn out to be 0.6 eV. This may be the correct picture and based on these arguments we can suggest that encapsulation of the acceptor fragment in α-CD results in a lowering of the outer shell reorganization energy by 0.1 eV (compared to that in pure water). Fukuzumi et al. reported results similar to this for photoinduced electron transfer between DNA-bound donors and intercalated acceptors.[22] For intramolecular photoinduced electron transfer in these systems, the reorganization energy was found to be reduced by 0.1 eV compared to that of the intermolecular process.

Visual demonstration of the inverted region: A very important aspect of the experimental design is that the raw fluorescence data obtained in this case provide a direct visual observation of the inverted region. Figure 8a–h shows the fluorescence decay profiles of PYCD in the presence of dif-

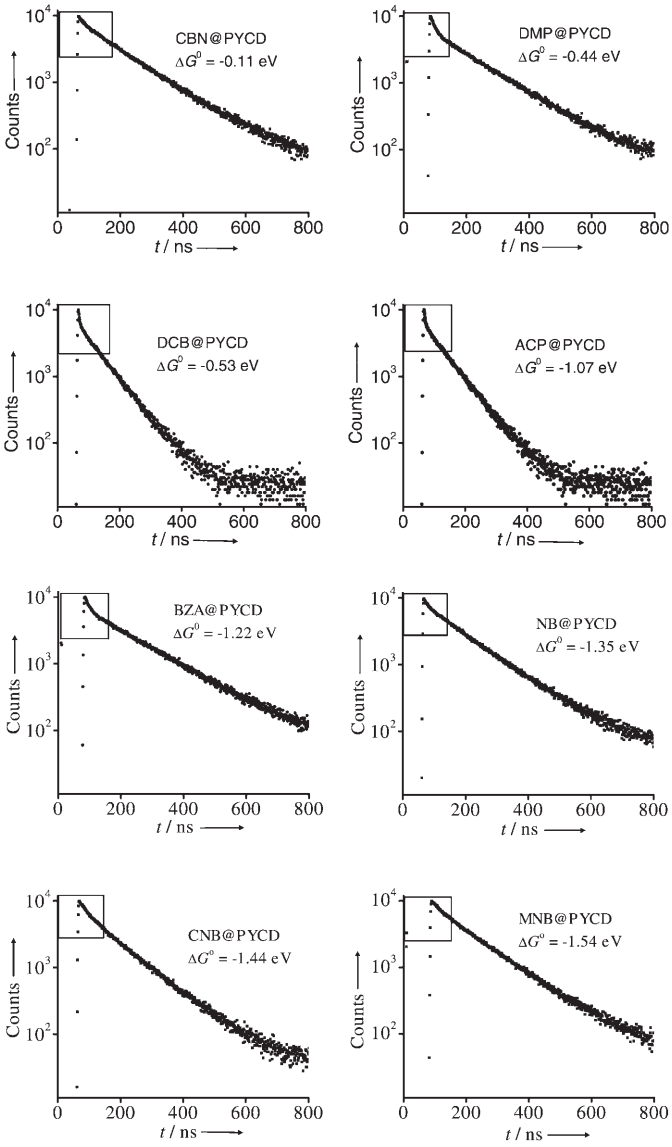

Figure 8. Fluorescence decay profiles of PYCD in the presence of different acceptors.

ferent acceptors arranged in the order of increasing driving force. Values of ΔG^0 are also shown in the plots. The biexponential nature of the fluorescence decays can be distinguished by the naked eye in all cases. The intra-ensemble PET rate constant k_{et} is obtained from the short lifetime component τ_1 as per Equation (4). As $1/\tau_1 \gg 1/\tau_0$ (see the Supporting Information), $k_{et} \approx 1/\tau_1$. This means that the faster the initial decay, the higher is the k_{et} value. An examination of the decay profiles (Figure 8a–h) reveals the following: as we proceed from a→b→c, the steepness of the initial decay component (shown in the box on the curve) increases, indicating that k_{et} increases from a→c. This corresponds to the normal region of the Marcus parabola. The steepness of the initial component is a maximum for c and d, indicating that these systems correspond to the top of the parabola. As we proceed further from d→e→f→g→h, the steepness of the initial component decreases, indicating that k_{et} decreases from d→h. This segment represents the inverted region. The experimental fluorescence profiles thus serve as a visual demonstration of the Marcus parabola in electron-transfer reactions (note that the acceptor concentrations are slightly different for the plots; however, this is immaterial because the short lifetime is independent of the acceptor concentration). The existence of an inverted region was the most important prediction of the Marcus theory, and definitive evidence for the inverted region was lacking for a long time.[14] Although the inverted region is now a well-established aspect of Marcus theory, papers dealing with the observation of an inverted region in newer systems continue to appear frequently in the current literature[22,23] (references [22] and [23] list only papers that have appeared in the last three years). Visual observation of the inverted region on the basis of raw experimental data, as presented here, has never been carried out before.

When log(counts) is plotted against time (or channel number), bimolecular decays can be clearly distinguished by the naked eye if $\tau_1 \ll \tau_2$. For systems at the bottom of the Marcus parabola, both in the normal and inverted regions, τ_1 is relatively large and the differences between τ_1 and τ_2 are small. In the inverted region, diffusion-mediated quenching is maximum, and hence τ_2 decreases rapidly with quencher concentration. This leads to further decreases in the difference between τ_1 and τ_2 in the inverted region. In the hydrogen-bonded systems studied earlier, $\tau_0 \approx 100$ ns and quencher concentrations required were in the 1–5 millimole range.[19] Because of this, the condition that $\tau_1 \ll \tau_2$ was achieved only for systems near the top of the Marcus parabola. In the present system with the cyclodextrin-appended pyrene, τ_0 is 204 ns and quencher concentrations employed were about ten times less. Because of this, the condition that $\tau_1 \ll \tau_2$ was achieved for all the systems studied and this enabled a visual observation of the Marcus parabola from the raw fluorescence lifetime data. Most of the earlier observations of the inverted region actually involved thermal electron-transfer reactions, which are generally not amenable to studies by fluorescence quenching.[15] In most of the published examples of the inverted region in intramolecular electron-transfer reactions, the bell-shaped function consisted of two distinct parts: i) a photoinduced forward process, which is restricted to the normal region, and ii) a thermal back-electron transfer, which is restricted to the inverted region. Thus, in these experiments, the Marcus parabola was built up from different types of experiments, the normal region constructed on the basis of fluorescence quenching experiments and the inverted region constructed from flash photolysis or pulse radiolysis experiments. Because of this, a visual demonstration of the inverted region could not be achieved from raw data. In our previous experiments with the hydrogen-bonded systems and also in the present system, the complete Marcus parabola was constructed from photoinduced forward electron-transfer reactions. In the present case, we are able to visually demonstrate the existence of the inverted region and also the total Marcus parabola on the basis of fluorescence decay curves and this constituted a very straightforward demonstration of the inverted region.

Conclusion

We have studied the free-energy dependence of PET reactions between α-cyclodextrin-appended pyrene and small acceptor molecules in aqueous solutions. A fraction of the acceptors associate with PYCD, leading to the formation of supramolecular dyads. Upon excitation, both unimolecular and diffusion-mediated electron transfers take place. The former component is attributed to electron transfer in the supramolecular dyad and this component followed the Marcus equation. The dynamic component is attributed to the freely diffusing PYCD and acceptors, and this component obeyed the Rehm–Weller equation. Similar to hydrogen-bonded systems, the CD-appended systems also enabled us to simultaneously observe Marcus and Rehm–Weller behaviors. The Marcus equation was used to determine donor–acceptor coupling and the reorganization energy in the supramolecular dyad systems. Electronic coupling was found to be similar to those reported for hydrogen-bonded systems. It appears that actual λ_{out} values are somewhat lower than calculated values. An important success of the study is that it enabled us to visually demonstrate the whole Marcus parabola on the basis of raw fluorescence lifetime data.

Experimental Section

Methods: NMR spectra were recorded on a 300 MHz Bruker Avance DPX spectrometer. MALDI mass spectrometry was conducted on a Perspective Biosystems Voyager DE PRO MALDI-TOF spectrometer in a matrix of α-cyano-4-hydroxybenzoic acid. Absorption spectra were recorded on a Shimadzu-3101PC UV/Vis/NIR scanning spectrophotometer. Fluorescence spectra were recorded on a SPEX Fluorolog F112X spectrofluorimeter. Fluorescence lifetimes were determined with an Edinburgh Instruments FL900CD single-photon counting system and the data were analyzed by Edinburgh software.

α-Cyclodextrin-appended pyrene (PYCD): This was synthesized by adopting a general procedure for the selective functionalization of a single primary OH of α-cyclodextrin.[7a] 1-Bromomethylpyrene (0.3 g, 1.05 mmol) was added to a solution of α-CD (1.0 g, 1.05 mmol) in 2,6-lutidine (90 mL), and the mixture was heated to 150 °C under an argon atmosphere for 3.5 h. Lutidine was then removed under vacuum, and the solid was washed several times with ethyl acetate and purified by chromatography (silica gel, methanol). It was purified by further chromatography (Sephadex column, deionized water). Yield of purified product was 30%. ^{1}H NMR (300 MHz, [D$_6$]DMSO, 25 °C, TMS): δ = 8.4–7.8 (m, 9H), 5.79–5.39 (m, 12H), 4.8 (s, 6H), 4.6–4.5 (m, 7H), 3.7–3.2 ppm (m, 36H); ^{13}C NMR (300 MHz, [D$_6$]DMSO, 25 °C, TMS): δ = 132.24, 131.69, 130.89, 130.75, 130.63, 130.47, 128.86, 128.51, 127.59, 127.09, 126.50, 125.96, 125.45, 124.83, 124.59, 124.02, 102.52, 102.10, 82.61, 82.22, 73.45, 73.05, 72.59, 72.23, 71.29, 71.02, 69.34, 60.68, 60.19 ppm; IR (KBr): $\tilde{\nu}$ = 3566, 2933, 2908, 2839, 1653, 1597, 1406, 1361, 1330, 1296, 1242, 1205, 1151, 1076, and 1033 cm^{-1}; UV/Vis (water): λ_{max} (ε) = 342 nm (43000 mol^{-1} dm^3 cm^{-1}); MS (MALDI-TOF): m/z: 1209.2 [M+Na]$^+$.

Quencher molecules: All quencher molecules were commercial samples from Aldrich. These were purified by standard methods before use. Stock solutions of acceptors were prepared as follows: a small amount (10–20 mg) of the acceptors were stirred in water for 2 h. These were then centrifuged and filtered. Concentrations of acceptors in the solution were estimated by means of the measured extinction coefficients in acetonitrile. Solutions used for the fluorescence lifetime experiments were deaerated by purging with argon for 20 min before use. The fluorescence lifetimes were measured with dilute solutions (OD ≈ 0.1 at the excitation wavelength 342 nm), and the emission was monitored at λ = 373 nm.

Acknowledgements

This work was supported by the Department of Science and Technology (DST), Government of India, New Delhi and the Council of Scientific and Industrial Research (CSIR Task Force Programme COR03), Government of India. B.B. thanks CSIR, Government of India, for a research fellowship. This is contribution No. RRLT-PPU-212 from the Photosciences and Photonics section of the Regional Research Laboratory, Trivandrum.

[1] a) J. L. Sessler, B. Wang, S. L. Springer, C. T. Brown in *Comprehensive Supramolecular Chemistry, Vol. 4* (Eds.: J. L. Atwood, J. E. D. Davies, D. D. MacNicol, F. Vögtle, Y. Murakami), Pergamon, Oxford, **1996**, pp. 311–336; b) M. D. Ward, *Chem. Soc. Rev.* **1997**, *26*, 365–375; c) P. Piotrowiak, *Chem. Soc. Rev.* **1999**, *28*, 143–150.

[2] *Electron Transfer in Chemistry, Vol. 3* (Ed.: V. Balzani), Wiley-VCH, Weinheim, **2001**.

[3] J. M. Haider, Z. Pikramenou, *Chem. Soc. Rev.* **2005**, *34*, 120–132.

[4] a) *Comprehensive Supramolecular Chemistry; Vol. 3* (Eds.: J. L. Atwood, J. E. D. Davies, D. D. MacNicol, F. Vögtle, J. Szejtli, T. Osa), Pergamon, Oxford, **1996**; b) J. Szejtli, *Chem. Rev.* **1998**, *98*, 1743–1754.

[5] a) A. Ueno, T. Osa in *Photochemistry in Organized and Constrained Media* (Ed.: V. Ramamurthy), VCH, New York, **1991** pp. 739–782; b) E. H. Yonemoto, G. B. Saupe, R. H. Schmehl, S. M. Hubig, R. L. Riley, B. L. Iverson, T. E. Mallouk, *J. Am. Chem. Soc.* **1994**, *116*, 4786–4795; c) H. Yonemura, H. Saito, S. Matsushima, H. Nakamura, T. Matsuo, *Tetrahedron Lett.* **1989**, *30*, 3143–3146; d) H. Yonemura, H. Nakamura, T. Matsuo, *Chem. Phys. Lett.* **1989**, *155*, 157–161; e) C. A. Chesta, D. G. Whitten, *J. Am. Chem. Soc.* **1992**, *114*, 2188–2197; f) M. Seiler, H. Duerr, I. Willner, E. Joselevich, A. Doron, J. F. Stoddart, *J. Am. Chem. Soc.* **1994**, *116*, 3399–3404; g) J. W. Park, B. A. Lee, S. Y. Lee, *J. Phys. Chem. B* **1998**, *102*, 8209–8215; h) H. Yonemura, S. Kusano, T. Matsuo, S. Yamada, *Tetrahedron Lett.* **1998**, *39*, 6915–6918; i) A. Masuhara, M. Fujitsuka, O. Ito, *Bull. Chem. Soc. Jpn.* **2000**, *73*, 2199–2206; j) T. Ito, T. Ujiie, M. Naka, H. Nakamura, *Chem. Phys. Lett.* **2001**, *340*, 308–316.

[6] a) Y. Kuroda, M. Ito, T. Sera, H. Ogoshi, *J. Am. Chem. Soc.* **1993**, *115*, 7003–7004; b) J. M. Haider, M. Chavarot, S. Weidner, I. Sadler, R. M. Williams, L. De Cola, Z. Pikramenou, *Inorg. Chem.* **2001**, *40*, 3912–3921; c) J. M. Haider, Z. Pikramenou, *Eur. J. Inorg. Chem.* **2001**, 189–194; d) H. F. M. Nelissen, M. Kercher, L. De Cola, M. C. Feiters, R. J. M. Nolte, *Chem. Eur. J.* **2002**, *8*, 5407–5414; e) Y.-H. Wang, H.-M. Zhang, Z.-X. Liang, L. Liu, Q.-X. Guo, C.-H. Tung, Y. Inoue, Y.-C. Liu, *J. Org. Chem.* **2002**, *67*, 2429–2434; f) Y.-H. Wang, Y. Fu, M.-Z. Zhu, X. Huang, Q.-X. Guo, *Res. Chem. Intermed.* **2003**, *29*, 11–19; g) Y.-H. Wang, M.-Z. Zhu, X.-Y. Ding, J.-P. Ye, L. Liu, Q.-X. Guo, *J. Phys. Chem. B* **2003**, *107*, 14087–14093; h) P. Silva, J. J. Maria, J. M. Haider, R. Heck, M. Chavarot, A. Marsura, Z. Pikramenou, *Supramol. Chem.* **2003**, *15*, 563–571; i) J. M. Haider, R. M. Williams, L. De Cola, Z. Pikramenou, *Angew. Chem.* **2003**, *115*, 1874–1877; *Angew. Chem. Int. Ed.* **2003**, *42*, 1830–1833.

[7] a) S. Tian, H. Zhu, P. Forgo, V. T. D'Souza, *J. Org. Chem.* **2000**, *65*, 2624–2630; b) A. R. Khan, P. Forgo, K. J. Stine, V. T. D'Souza, *Chem. Rev.* **1998**, *98*, 1977–1996.

[8] a) A. Makabe, K. Kinoshita, M. Narita, F. Hamada, *Anal. Sci.* **2002**, *18*, 119–124; b) M. Narita, S. Mima, N. Ogawa, F. Hamada, *Anal. Sci.* **2001**, *17*, 379–386; c) F. Hamada, M. Narita, K. Kinoshita, A. Makabe, T. Osa, *J. Chem. Soc. Perkin Trans. 2* **2001**, 388–394; d) A. Ueno, I. Suzuki, T. Osa, *Anal. Chem.* **1990**, *62*, 2461–2466; e) A. Ueno, I. Suzuki, T. Osa, *J. Am. Chem. Soc.* **1989**, *111*, 6391–6397.

[9] K. Kano, I. Takenoshita, T. Ogawa, *J. Phys. Chem.* **1982**, *86*, 1833–1838.

[10] a) C. K. Mann, K. B. Barnes, *Electrochemical Reactions in Nonaqueous Systems*, Marcel Dekker, New York, **1970**; b) M. Fagnoni, M. Mella, A. Albini, *J. Org. Chem.* **1998**, *63*, 4026–4033.

[11] a) M. Julliard in *Photoinduced Electron Transfer, Part B*, (Eds.: M. A. Fox, M. Channon), Elsevier, New York, **1988**, pp. 216–313; b) G. P. Zanini, H. A. Montejano, C. M. Previtali, *J. Chem. Soc. Faraday Trans.* **1995**, *91*, 1197–1202; c) J. E. Baggot, M. J. Pilling, *J. Chem. Soc. Faraday Trans. 1*, **1983**, *79*, 221–234; d) T. Hino, H. Akazawa, H. Masuhara, N. Mataga, *J. Phys. Chem.* **1976**, *80*, 33–37; e) A. Tsuchida, M. Yamamoto, Y. Nishijima, *J. Phys. Chem.* **1984**, *88*, 5062–5064.

[12] a) M. V. Rekharsky, Y. Inoue, *Chem. Rev.* **1998**, *98*, 1875–1918; b) K. A. Connors, D. D. Pendergast, *J. Am. Chem. Soc.* **1984**, *106*, 7607–7614; c) L. Liu, Q.-X. Guo, *J. Phys. Chem. B* **1999**, *103*, 3461–3467.

[13] J. W. Park, H. E. Song, S. Y. Lee, *J. Phys. Chem. B* **2002**, *106*, 7186–7192.

[14] a) R. A. Marcus, P. Siders, *J. Phys. Chem.* **1982**, *86*, 622–630; b) P. Siders, R. A. Marcus, *J. Am. Chem. Soc.* **1981**, *103*, 741–747; c) R. A. Marcus, N. Sutin, *Biochim. Biophys. Acta* **1985**, *811*, 265–322; d) N. Sutin, *Acc. Chem. Res.* **1982**, *15*, 275–282.

[15] P. Suppan, *Top. Curr. Chem.* **1992**, *163*, 95–130, and references therein.

[16] a) D. Rehm, A. Weller, *Ber. Bunsen-Ges. Phys. Chem.* **1969**, *73*, 834–839; b) D. Rehm, A. Weller, *Isr. J. Chem.* **1970**, *8*, 259–271.

[17] G. J. Kavarnos, *Fundamentals of Photoinduced Electron Transfer*, VCH, New York, **1993**, pp. 62.

[18] AM1 calculations of the molecular length were carried out with Titan Version 1 from Wavefunction Inc.; 18401, Von Karman, Suite 370, Irvine, CA 92612, USA.

[19] a) E. Prasad, K. R. Gopidas, *J. Am. Chem. Soc.* **2000**, *122*, 3191–3196; b) M. A. Smitha, E. Prasad, K. R. Gopidas, *J. Am. Chem. Soc.* **2001**, *123*, 1159–1165.

[20] a) D. A. Williamson, B. E. Bowler, *J. Am. Chem. Soc.* **1998**, *120*, 10902–10911; b) T. H. Ghaddar, E. W. Castner, S. S. Isied, *J. Am. Chem. Soc.* **2000**, *122*, 1233–1234.

[21] a) R. A. Marcus, *J. Chem. Phys.* **1956**, *24*, 966–978; b) R. A. Marcus, *Annu. Rev. Phys. Chem.* **1964**, *15*, 155–196.

[22] a) S. Fukuzumi, M. Tanaka, M. Nishimine, K. Ohkubo, *J. Photochem. Photobiol. A* **2005**, *175*, 79–81; b) S. Fukuzumi, M. Nishimine,

K. Ohkubo, N. V. Tkachenko, H. Lemmetyinen, *J. Phys. Chem. B* **2003**, *107*, 12511–12518.

[23] a) S. A. Vail, P. J. Krawczuk, D. M. Guldi, A. Palkar, L. Echegoyen, J. P. C. Tomé, M. A. Fazio, D. I. Schuster, *Chem. Eur. J.* **2005**, *11*, 3375–3388; b) G. A. Rajkumar, A. S. D. Sandanayaka, K.-i. Ikeshita, M. Itou, Y. Araki, Y. Furusho, N. Kihara, O. Ito, T. Takata, *J. Phys. Chem. A* **2005**, *109*, 2428–2435; c) P. A. Liddell, G. Kodis, D. Kuciauskas, J. Andréasson, A. L. Moore, T. A. Moore, D. Gust, *Phys. Chem. Chem. Phys.* **2004**, *6*, 5509–5515; d) A. M. Ramos, E. H. A. Beckers, T. Offermans, S. C. J. Meskers, R. A. J. Janssen, *J. Phys. Chem. A* **2004**, *108*, 8201–8211; e) E. H. A. Beckers, S. C. J. Meskers, A. P. H. J. Schenning, Z. Chen, F. Würthner, R. A. J. Janssen, *J. Phys. Chem. A* **2004**, *108*, 6933–6937; f) L. R. Sutton, M. Scheloske, K. S. Pirner, A. Hirsch, D. M. Guldi, J.-P. Gisselbrecht, *J. Am. Chem. Soc.* **2004**, *126*, 10370–10381; g) D. I. Schuster, P. Cheng, P. D. Jarowski, D. M. Guldi, C. Luo, L. Echegoyen, S. Pyo, A. R. Holzwarth, S. E. Braslavsky, R. M. Williams, G. Klihm, *J. Am. Chem. Soc.* **2004**, *126*, 7257–7270; h) A. Chakraborty, D. Chakrabarty, P. Hazra, D. Seth, N. Sarkar, *Chem. Phys. Lett.* **2004**, *387*, 517–517; i) M. Kumbhakar, S. Nath, T. Mukherjee, H. Pal, *J. Chem. Phys.* **2004**, *120*, 2824; j) D. R. Worrall, I. Kirkpatrick, S. L. Williams, *Photochem. Photobiol. Sci.* **2004**, *3*, 63; k) K. G. Thomas, V. Biju, P. V. Kamat, M. V. George, D. M. Guldi, *ChemPhysChem* **2003**, *4*, 1299–1307; l) K. Yamanaka, M. Fujitsuka, Y. Araki, O. Ito, T. Aoshima, T. Fukushima, T. Miyashi, *J. Phys. Chem. A* **2004**, *108*, 250–256; m) P. Sun, F. Li, Y. Chen, M. Zhang, Z. Zhang, Z. Gao, Y. Shao, *J. Am. Chem. Soc.* **2003**, *125*, 9600–9601; n) A. Chakraborty, D. Chakrabarty, P. Hazra, D. Seth, N. Sarkar, *Chem. Phys. Lett.* **2003**, *382*, 508–517; o) D. M. Guldi, A. Hirsch, M. Scheloske, E. Dietel, A. Troisi, F. Zerbetto, M. Prato, *Chem. Eur. J.* **2003**, *9*, 4968–4979; p) M. Yasuda, R. Kojima, H. Tsutsui, D. Utsunomiya, K. Ishii, K. Jinnouchi, T. Shiragami, T. Yamashita, *J. Org. Chem.* **2003**, *68*, 7618–7624; q) M. Kumbhakar, S. Nath, H. Pal, A. V. Sapre, T. Mukherjee, *J. Chem. Phys.* **2003**, *119*, 388–399; r) D. M. Guldi, C. Luo, N. A. Kotov, T. Da Ros, S. Bosi, M. Prato, *J. Phys. Chem. B* **2003**, *107*, 7293–7298; s) M. Fujitsuka, N. Tsuboya, R. Hamasaki, M. Ito, S. Onodera, O. Ito, Y. Yamamoto, *J. Phys. Chem. A* **2003**, *107*, 1452–1458; t) S. Fukuzumi, *Org. Biomol. Chem.* **2003**, *1*, 609–620; u) S. Fukuzumi, K. Ohkubo, H. Imahori, D. M. Guldi, *Chem. Eur. J.* **2003**, *9*, 1585–1593.

Received: December 12, 2005
Revised: March 3, 2006
Published online: June 26, 2006

